Chapter 4
Parametric Sizing Optimization

This chapter details the parametric sizing optimization of an aircraft spoiler subjected to both performance and manufacturing constraints. A practical optimization problem was formulated to find the absolute lightest spoiler subject to manufacturing constraints and operational restrictions on stiffness. Design requirements were expressed mathematically and met with sizing optimization. Manufacturing constraints were enforced by human input and were de-coupled from the sizing optimization. The geometry, boundary conditions and loading conditions were equivalent to those presented in Chapter 2. The optimization methodology presented can be applied to any thin-walled structure.

4.1 Introduction

4.1.1 Spoiler Design Assumptions

The generic spoiler design problem presented in Chapter 2 is revisited in this chapter. However, unlike the previous chapter, some explicit assumptions are made about the manufacturing processes to be used. Firstly, it was assumed that the spoiler is manufactured from thin panels joined with rivets. Also, flanges were included on the interior members for connection to the skin. These flanges were also incorporated into the FEA used during this work. This construction method is common for the primary and secondary structure in almost all categories of aircraft.

The optimization search space involves the layout of the internal members and the thickness of both the internal and external (skin) panels. A non-buckling design was sought to keep the computational costs manageable. To approach the minimum weight structure, non-orthogonal internal members were allowed in candidate designs.

Hence, no restriction was placed on members being parallel to or perpendicular to the main spar.

4.1.2 Sizing Optimization

Sizing Optimization seeks the optimal adjustments to a design for applied loads and performance constraints such as stress, stiffness, buckling etc. The method of sizing optimization often uses computer models and involves mathematical programming (Vanderplaats, 1984, Grooms *et al.*, 1992), heuristics (Chu *et al.*, 1998) or human intuition. It involves repeated analyses with variations made to dimensional variables of the design. Sizing variables can be of various types (Ashley, 1982); panel thickness, beam cross-sectional area, location variables, etc.

Since sizing optimization varies only the dimensions of a design, it fixes the design's configuration (or topology) and can limit the design space. Hence, in this study sizing optimization was not used to define the internal structural layouts for the spoiler. Rather, sizing optimization was used as a second step to refine candidate designs to meet structural performance criteria.

4.1.3 Group ESO

Group ESO by Lencus *et al.* (1999) is an extension of the method of Evolutionary Structural Optimisation (ESO) by Xie & Steven (1993). Group ESO involves the removal of under stressed finite elements from a structural model by an algorithm similar to conventional ESO. However, Group ESO enforces the condition of *group removal* whereby groups of finite elements are removed rather than individual elements. In this way, more manufacturable designs are obtained by restricting the arrangement of the groups. Thus, Group ESO can provide structurally efficient starting points for configuration selection. In this work, it was used to determine one

of the multiple trial configurations that are discussed later in this chapter. The Group ESO optimization problem was started from a design with a wide range of angled and orthogonal ribs. These ribs were modeled as groups of vertical shell elements running fully across the interior of the spoiler (Figure 4.1).

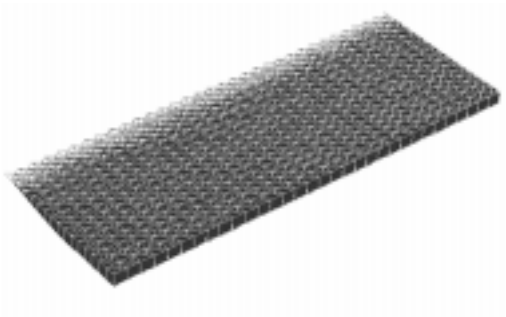

Figure 4.1, Initial design used for Group ESO.

Group ESO suggested a design concept that was both structurally efficient and manufacturable. In this instance, the groups were removed according to the average stress in the group although a variety of other criteria can be used to drive the optimization. Figure 4.2 shows the optimized design. This result was one of many to be compared later in this study.

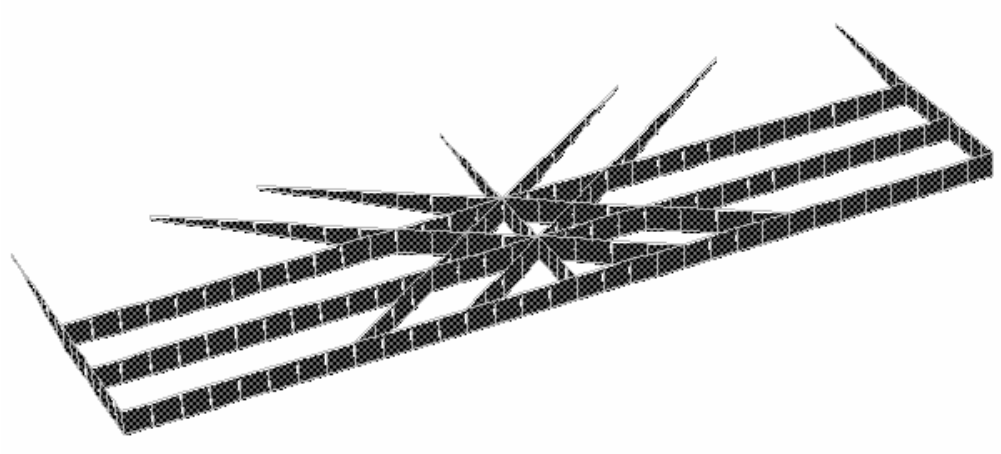

Figure 4.2, Optimal design suggested by the Group ESO method.

4.2 Methodology

The most significant contribution of the research presented in this chapter was the demonstration of a practical problem formulation for optimizing the design of a spoiler. The approach addressed both real-world issues and the capabilities of available software.

4.2.1 Problem Formulation

To allow for manufacturing of the optimized spoiler, two classes of constraints were essential. Firstly, the deformations of the spoiler were constrained to ensure a sufficiently stiff structure. Secondly, the design was constrained to be manufacturable. The problem was formulated as follows:

Minimize the weight of the spoiler described above, subject to the following constraints:

$$\begin{aligned} &\delta_{MAX} \leq 10mm \\ &\lambda_{MIN} \geq 1.0 \\ &Design\ \ can\ \ be\ \ maufactured \end{aligned} \qquad (4.1)$$

where δ_{MAX} is the maximum linear static deflection anywhere on the structure, λ_{MIN} is the lowest buckling eigenvalue and the manufacturing constraint excludes any designs that cannot be manufactured (designs requiring only small alterations were considered to be acceptable).

The first two constraints in (4.1) relate to the performance of the structure under load and were evaluated through computations. The third constraint relates to manufacturing and was satisfied by human interpretation of the feasibility of

manufacturing the design using a known technique. Hence, designs with excessively complex panel intersections, members in close proximity, etc., were not considered. The Group ESO design of Figure 4.2 represents the upper limit in manufacturing complexity that was allowed in this study.

Since the spoiler's role on the aircraft is to control the airflow around the wing, the dominant design requirement is a small deflection at the tip. However, the deflection constraint was applied to the entire structure to avoid geometrically non-linear deformations in the relatively thin skins of the spoiler. This small deflection constraint led to stress levels in the structure well below the material yield point and hence no stress constraints were required.

The buckling constraint was included to ensure that the linear static deformations were valid. This excluded designs with post-buckling behaviour from the search space. In future studies, non-linear geometric analyses could be employed to include post-buckling designs. However, a large increase in computational expense would be expected.

4.2.2 Optimization Approach

The approach sought a synergy between the sizing and topology optimization methods while including human intuition in the design process. This was achieved by sizing optimizations of multiple trial configurations. As such, the design process was not restricted to one structural configuration or topology. Figure 4.3 contains a flow chart detailing the procedure used in this study.

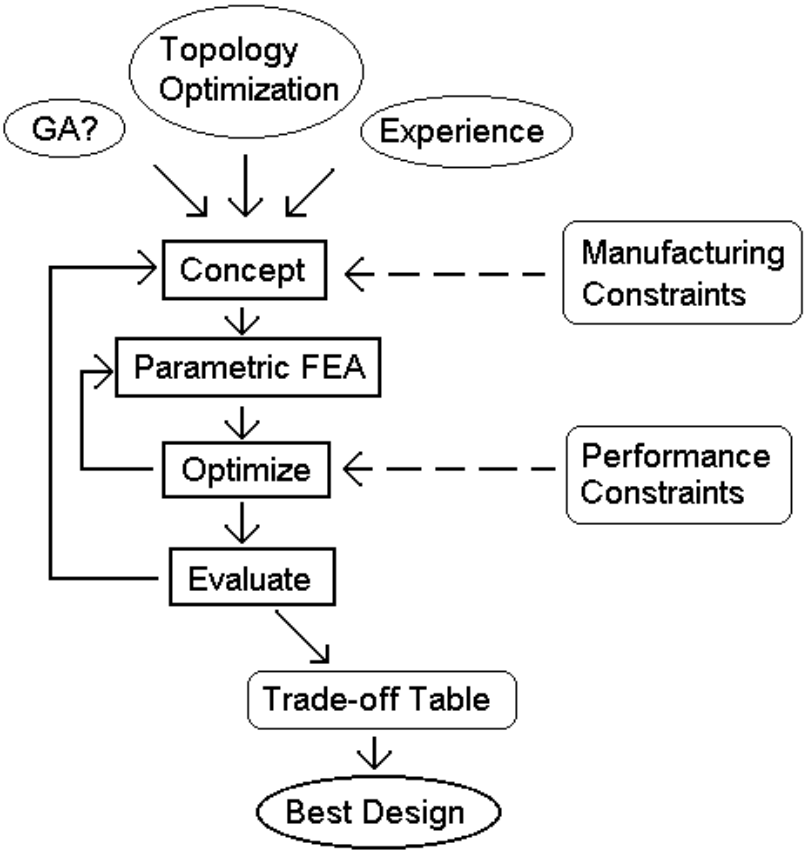

Figure 4.3, Flow chart describing the optimization procedure.

The process began with the choice of concepts using a variety of inputs. The ellipse containing 'Experience' represents human input to the design process. 'Topology Optimization' was another input to the choice of concept and the Group ESO result was used as the input for this study. As an alternative, the entire process could become fully automated with a Genetic Algorithm (Goldberg, 1989) to drive the choice of concept. The 'GA' ellipse indicates this option although its use was beyond the scope of this work. Rudimentary computer models that included the locations of internal members (but no sizing information) were used to represent the 'Concept' data.

Since the manufacturing constraints were non-mathematical, they were addressed at the concept stage with human input to ensure that the trial configurations could be

manufactured. This de-coupled the manufacturing issues from the mathematical programming based optimization in later steps. Such de-coupling is valid for multi-component panel structures because manufacturing feasibility is mostly unaffected by panel thicknesses.

After computer models for each of the concepts were created, they were subjected to separate sizing optimizations to select optimal thicknesses for the internal members and skins. This sizing optimization was achieved by parametric FEA modeling in an optimization loop. The ‘Parametric FEA’ and ‘Optimize’ boxes represent the sizing optimization loop and the ‘Performance Constraints’ box indicates the inclusion of the mathematical performance constraints in the optimization.

After sizing optimization for each configuration concept was completed, the weight and number of stiffening panels were entered into a trade-off table. The number of panels was intended as a rough indicator of manufacturing complexity. The designer makes a selection of the best design after all trial configurations have been added to the trade-off table.

4.3 Computations

The ANSYS commercial FEA package was chosen for modeling and optimizing the trial configurations due to its parametric modeling and in-built optimization algorithms. Each analysis involved a linear static solution and a linear buckling solution of models containing predominantly shell elements. State variables for the optimization were maximum deflection in the linear static solution and buckling load factor from the linear buckling solution. The objective function to be minimized was the weight of the spoiler model.

4.3.1 Modeling Approximations

To keep computational costs low, a number of approximations were made. Firstly, the stiffness and weight contributions of the flanges were approximated with beam elements along the panel edges. The thickness of the flanges was linked to the corresponding panels and the flange width was set at 20mm. Secondly, the ANSYS automatic meshing was used with a desired side length of 50mm. Elements of this size are unlikely to give highly accurate linear buckling calculations so an extra factor of 1.2 was used for the buckling load constraint. This factor could be regarded as a factor of safety. The third approximation relates to the three trial configurations containing stiffeners (discussed below). These stiffeners were assumed to be blade stiffeners with flanges. The stiffener flanges were modeled with beams in the same manner as the panel flanges.

4.3.2 ANSYS Optimizer settings

The in-built optimizer in ANSYS includes a variety of optimization algorithms that work in the absence of user supplied sensitivities. Where required, ANSYS evaluates design variable sensitivities by finite difference. With this arrangement, the flexibility of batch file analysis is available but convergence of the optimization problems is slower than with other software. Additionally, ANSYS provides a built-in method for constraining response variables such as maximum deflection or the minimum buckling load factor.

Initially, the in-built constraint method was used for both buckling and deflection. Using this method, ANSYS was unable to converge on solutions with a buckling load factor near the constraint value. Hence, the ANSYS optimizer solutions were overweight because they exceeded the requirements on buckling. This problem existed for both the zero-order (sub-problem approximation) and first-order (finite

difference gradient method) optimization algorithms. It was presumed that a non-linear relationship between panel thicknesses and buckling location affected the convergence of the buckling load. To achieve results, a different method of constraining buckling was required. A weight penalty was introduced for designs that buckled below the desired load factor of 1.2. The buckling penalty was evaluated as follows:

$$Obj = \begin{cases} Mass + \omega \dfrac{(1.2 - F_{CR})}{1.2} & F_{CR} < 1.2 \\ Mass & F_{CR} \geq 1.2 \end{cases} \qquad (4.2)$$

where Obj was the objective function to be minimized, $Mass$ was the mass of the spoiler model, ω was the maximum buckling penalty (typically 5 kg) and F_{CR} was the lowest buckling load factor from the linear buckling analysis.

With buckling constrained by (4.2), the zero-order optimization algorithm was still unable to converge so the first-order optimization algorithm was required. The use of a penalty method and the first-order algorithm increased the number of optimization cycles but did provide converged results. Since the first-order algorithm is gradient based, there is no guarantee that the global optima were reached for each of the candidate configurations.

4.4 Trial Configurations

Figure 4.4 shows schematics of the interior structural layouts for all the trial concepts that were considered[1].

[1] The spoiler configuration suggested by the 3D topology optimization work in Chapter 2 was not considered in this parametric study since it was actually done a year later as part of a research exchange at the University of Tokyo, after expiry of the ANSYS software licensing agreement. These two research activities were introduced in reverse order for reasons of continuity of this thesis.

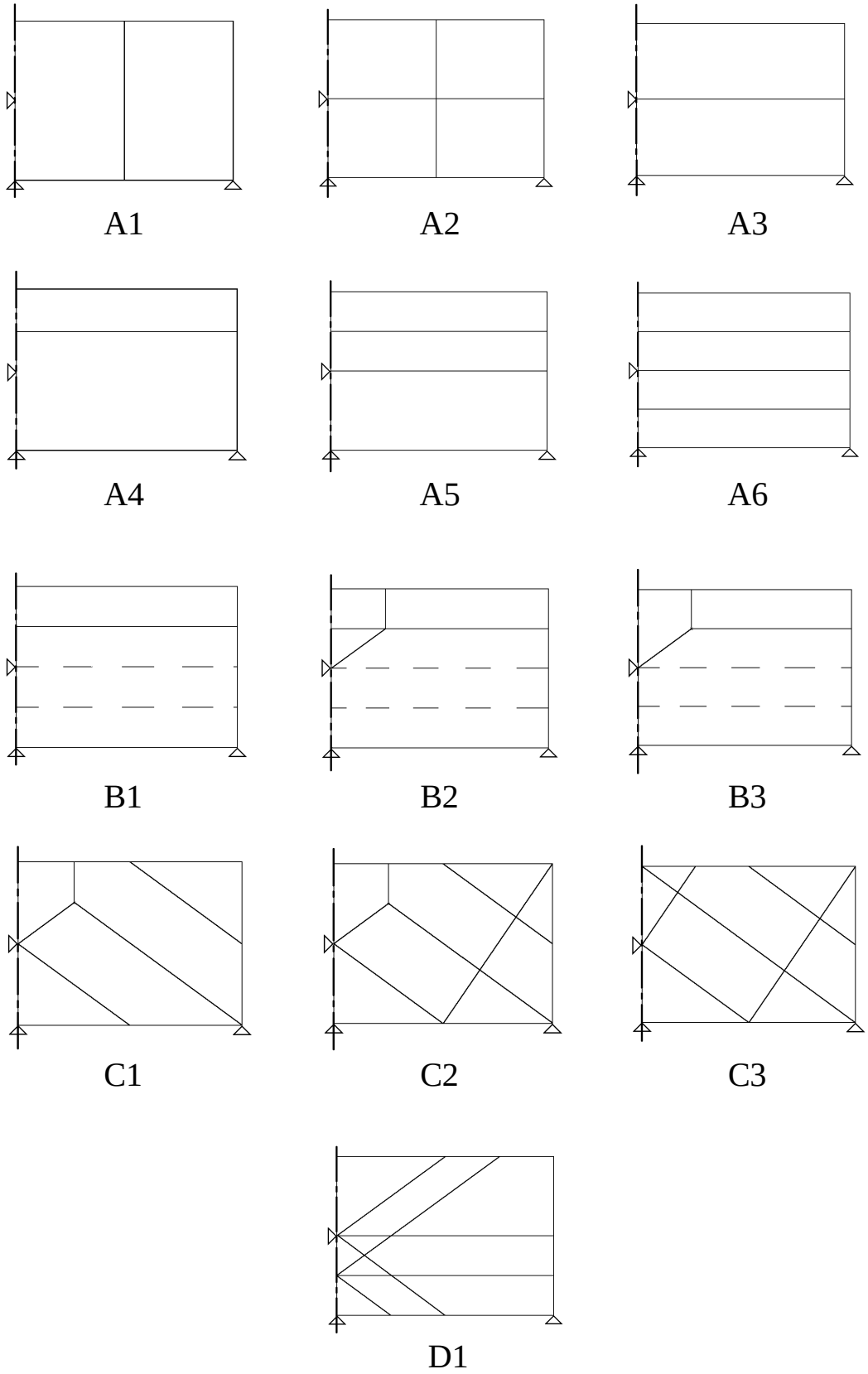

Figure 4.4, Interior structural schematics for trial concepts

(due to symmetry, only the right half of the schematics are shown).

Due to symmetry, only the right half of the schematics are shown (symmetry axis on left side of schematics). Each of the lines represents an internal member that is attached to the top and bottom skins with flanges. The hinge and actuator locations are also marked with triangles. Concepts beginning with the letter 'A' were chosen to reflect the common design practice of internal members in an orthogonal arrangement. The designs beginning with 'B' included stiffeners on the top and bottom skins. The locations of the stiffeners are designated with the dashed lines. Those beginning with letter 'C' were generated from aligning members with load flow distributions in an equivalent flat plate model (not shown here). The 'D1' concept was produced by Group ESO as mentioned earlier.

Between 5 and 10 panel thickness parameters were included when optimizing each of the configurations. The panel thickness variables were allowed to range from 0.4mm to 10mm. However, 10mm was far more than required. The designs containing stiffeners were assigned extra parameters for stiffener heights and thicknesses. The maximum height of the stiffeners was 30mm for the top skin and 20mm for the bottom skin. For both sets of stiffeners, the minimum height was set at 5mm.

4.5 Results

Table I shows the optimized volumes for each of the configurations. As a rough estimate of relative manufacturing cost, the number of uninterrupted internal panels was used. The numbers in the right column of Table 4.1 were found by counting the number of uninterrupted[2] interior line segments on the symmetric layouts in Figure 4.4.

[2] This can be taken to mean all lines are discontinuous at their intersections with other lines in the 2D drawings.

Concept	Weight (kg)	Internal members
A1	6.67	1
A2	6.30	4
A3	6.49	1
A4	7.03	1
A5	6.44	2
A6	6.07	3
B1	4.67	5
B2	4.89	8
B3	5.07	7
C1	4.48	5
C2	3.96	10
C3	4.37	11
D1	4.28	12

Table 4.I, Trade-off table of trial concepts.

The lightest design was ‘C2’ at 3.96 kg and the heaviest was ‘A4’ at 7.03 kg. The designs with the least internal panels were all in the ‘A’ category while ‘D1’ had the most. Figure 4.5 shows a significant correlation between number internal members and lower weight.

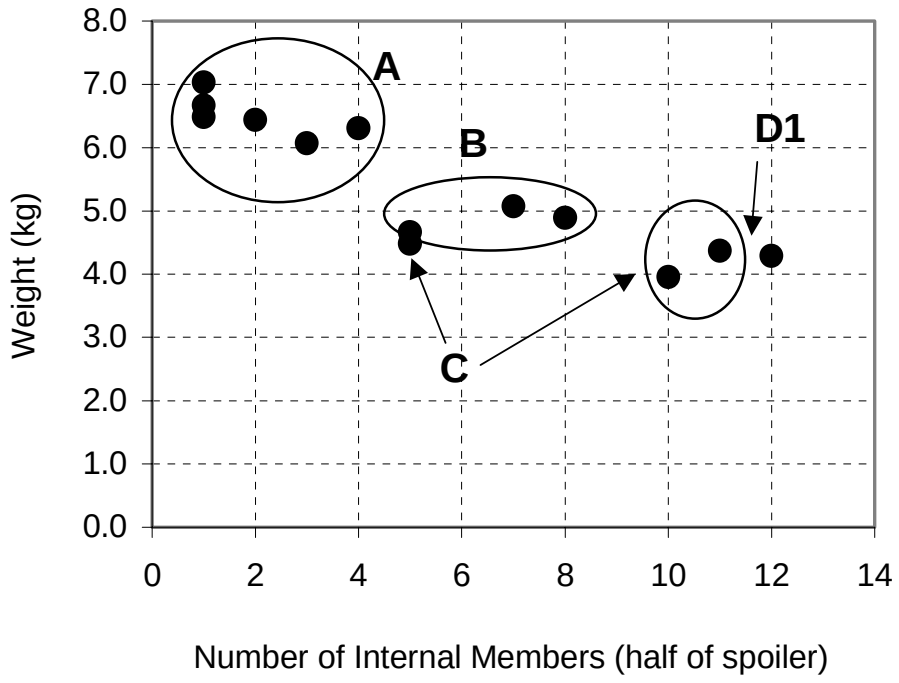

Figure 4.5, Correlation plot of trial concepts

4.6 Conclusion

The practical application of sizing optimization has been demonstrated on the design of an aircraft spoiler. The configuration of the design was optimized rather than the sizing details of an individual configuration. It was shown that the manufacturing issues could be treated during structural optimization if they are de-coupled from the sizing optimization phases.

Two factors were recognised as contributing to efficient interior structural layouts under the objectives set out in Equation (4.1). Firstly, the maximum linear static deflections usually occurred in the largest unsupported skin region on the top skins of the models. This suggests that the size of the largest unsupported region influenced the weight of the optimized models. However, if the size of the unsupported regions

alone accounted for the optimal arrangement, the orthogonal design ‘A6’ should have performed as well as the angled design ‘C1’. Hence there were other factors contributing to efficient rib arrangements. One other influence on the internal layout was the linear buckling constraint. This constraint penalized the orthogonal arrangements more than the non-orthogonal ones. By design, these non-orthogonal arrangements all tended to reflect the load flow through the structure – as evaluated by human interpretation of an equivalent plate model in the ‘C’ designs or by Group ESO in ‘D1’. Hence, arranging interior members along the load paths was most efficient for buckling performance.

The various design categories are seen to cluster in certain regions of the design space of Figure 4.5. The ‘A’ category designs with orthogonal members reside in the heavier and less complex region whereas the angled rib designs of categories ‘C’ and ‘D’ reside in the lighter but more complex region. Such clustering is an intuitive result that reflects the underlying trade-off between weight savings and manufacturing complexity.

Using the approach described by the flowchart in Figure 4.3, the number of trial configurations is limited only by the imagination of the designer. Only a small number of configurations (13) were covered here so the existence of a design that is even lighter than ‘C2’ is inevitable. Although more complex to manufacture, the apparent weight savings suggested that non-orthogonal members should be considered in trade-off studies. Since manufacturing considerations often dominate the choice of configuration, the feasibility of manufacturing the ‘C2’ option needs to be addressed in future work. Also, due to the constraint on linear buckling, the optimal post-buckled design remains to be seen.

References

Ashley, H., “On Making Things the Best – Aeronautical Uses of Optimization”, *Journal of Aircraft*, Vol. 19 No.1, pp. 5-28, 1982.

Bendsøe, M. P., Kikuchi, N., “Generating optimal topologies, in structural design using the homogenization method”, *Comp. Meth. Appl. Mech. Eng.*, Vol. 71, pp. 197-205, 1988.

Chu, D. N., Xie, Y. M., Steven, G. P., “An evolutionary structural optimization method for sizing problems with discrete design variables”, *Computers and Structures*, Vol. 68, pp. 419-431, 1998.

Goldberg, D. E., *Genetic Algorithms in Search, Optimization and Machine Learning*, Addison-Wesley, Reading, MA, 1989.

Grooms, H. R., DeBarro, C. F., Paydarfar, S., “What is an Optimal Spacecraft Structure?”, *Journal of Spacecraft and Rockets*, Vol. 29, No. 4, pp. 480-3, 1992.

Lencus, A., Querin, O. M., Steven, G. P., Xie, Y. M., “Group ESO with morphing”, *Proc. 1’st ASMO UK/ISSMO conf. of engineering design optimization*, Ilkley, UK, 1999.

Lencus, A., Querin, O. M., Steven, G. P., Xie, Y. M., “Modifications to the evolutionary structural optimisation (ESO) method to support configurational optimisation”, *Proceedings WCSMO-3*, Buffalo, USA, 1999.

Ness, R., Wang, J., Kelly, D., Raju, J., Barton, A., Lindsay, A., “Conceptual Design of a Wing Spoiler”, *Proc. Second Australasian Congress on Applied Mechanics*, Canberra, Australia, 1999.

Vanderplaats, G. N., *Numerical Optimization Techniques for Engineering Design: With Applications*, McGraw-Hill, New York, 1984.

Xie, Y. M., Steven, G. P., “A simple evolutionary method for structural optimization”, *Computers and Structures*, Vol. 49, pp. 885-886, 1993.